Applied Surface Science 258 (2012) 8831–8836

Contents lists available at SciVerse ScienceDirect

Applied Surface Science

journal homepage: www.elsevier.com/locate/apsusc

Effects of interactions between NiM (M = Mn, Fe, Co and Cu) bimetals with MgO (1 0 0) on the adsorption of CO_2

Baojun Wang[a,*], Ruixia Yan[a], Hongyan Liu[a,b]

[a] Key Laboratory of Coal Science and Technology of Ministry of Education and Shanxi Province, Taiyuan University of Technology, Taiyuan 030024, China
[b] College of chemistry and Chemical Engineering, Shanxi Datong University, Datong 037009, Shanxi Province, China

ARTICLE INFO

Article history:
Received 31 October 2011
Received in revised form 20 May 2012
Accepted 20 May 2012
Available online 27 May 2012

Keywords:
Metal–support interaction
CO_2 adsorption
Density functional theory

ABSTRACT

A density-functional theory method has been conducted to investigate the interactions of NiM (M = Mn, Fe, Co and Cu) with MgO (1 0 0) as well as the effects of interactions on the adsorption of CO_2. The binding energies of NiM on MgO and the adsorption energies of CO_2 on NiM/MgO have been calculated, and the results show that the defective NiM/MgO catalysts exhibit stronger metal–support interaction (MSI) than the perfect NiM/MgO catalysts do, leading to weaker adsorption ability to CO_2, except NiMn/MgO system. However, for the catalysts with the same MgO surface and different bimetals, the stronger the MSI is, the stronger adsorption ability of the substrate to CO_2 is, except NiCu/MgO system.

1. Introduction

It has always been a hot topic in recent years that catalytic reforming of CH_4 with CO_2 to produce synthesis gas [1–7]. This process not only reduces greenhouse gas emission, but also produces synthesis gas with the ratio to unit which is more preferable feeds for some liquid fuel synthesis processes. Metal Ni, because of its good activity and relatively low cost, is selected as the catalyst in the reforming reaction. However, a serious problem, carbon of coke formation, made Ni catalysts deactivate and restricted the industrialization process [8,9]. Fortunately, the O species [10,11] from CO_2 dissociation may interact with the formed carbon to reduce the carbon deposition. Therefore, CO_2 dissociation is an important step in CH_4/CO_2 reforming reaction. Further, the adsorption of CO_2 is an initial step for dissociation process. A detailed mechanism for adsorption of CO_2 at the molecular level can help us to better understand the key factors that affect the performance of the catalysts to remove carbon.

Several studies have shown that bimetallic systems have certain characteristics that make them better catalysts than the corresponding pure metals because of their better activation, stability and selectivity [12,13]. Besenbacher et al. [14,15] found that alloying Ni catalysts with small amounts of gold can greatly reduce coking. Pt-Ni/MCM-41 has also been reported that it has excellent performance in hindering carbon formation [16]. Wang and co-workers [17] have compared four bimetallic catalysts systems Ni-M-Al_2O_3-MgO (M = Mn, Fe, Co and Cu), and concluded that Ni-Co bimetallic catalyst has superior performance in terms of activity and stability compared to other Ni-M combinations, which resulted from not only the synergy between Ni and Co, but also strong metal–support interaction (MSI). Other studies have also confirmed that formed carbon can be reduced when strong MSI exists in the catalyst [18–20]. This effect is determined both by characters of support surface and metal [21].

MgO has often been used as a support for dispersed metal particles owing to its relatively well-defined surface structure and stoichiometry [22]. More importantly, it is easy to form defects on the MgO surface, which can show strong MSI, and further have a direct influence on the properties of adsorbed species [23–25]. For example, Markovits and co-workers [26] compared the adsorption of the first transition metal row on the regular and defective MgO (1 0 0) surfaces, and they found Co, Ni and Cu atoms all exhibit higher adsorption energies apparently on the defective surfaces. Wang et al. [24,27] also got the similar conclusion using both cluster and embedded cluster models. Ferrari et al. [28] have found that only when Pd atoms bound to defect sites, do they become catalytically active for reactions, which is mainly due to the electrons transfer from the cavity to the supported metal [24,29,30]. Further, the effect of defective MgO with metals on adsorption characteristic to small molecules has also been studied. Fuente et al. [31] studied the adsorption of NO on single gold atom and Au_2 dimmer deposited on the perfect surface and the oxygen vacancy surface of MgO using cluster models. It was found that the adsorption of NO is stronger when the Au atom is supported on a perfect site than when it is on a defect

* Corresponding author. Tel.: +86 351 6018539.
E-mail addresses: wangbaojun@tyut.edu.cn, wangbaojuntyut@163.com (B. Wang).

0169-4332/$ – see front matter © 2012 Elsevier B.V. All rights reserved.
http://dx.doi.org/10.1016/j.apsusc.2012.05.100

site, while the NO molecules bonds weakly with Au_2 both on the two substrates. To the best of our knowledge, a few studies about support MgO are based on the periodic model [32], and the active components are single atom or dimmer basically. However, for Ni-based bimetals active components, few investigations are reported, although they have been used broadly in experiment. Furthermore, there is no conclusion to distinguish the degree of interaction between MgO and different Ni-based bimetals both in experimental and theoretical studies. In addition, studies about the effects of defective MgO supported bimetals on CO_2 adsorption are seldom.

In the present work, we carry out a density functional theory (DFT) calculations with periodic slab model on the interactions between Ni-based bimetals (NiMn, NiFe, NiCo and NiCu) and MgO surfaces as well as their effects on CO_2 adsorption. Our aims are: (1) to study the effects of oxygen vacancy on the interactions of MgO with NiM and the adsorption ability of NiM/MgO to CO_2; (2) to study which bimetal shows the strongest interaction with surface and which bimetal system shows the strongest adsorption characteristic to CO_2; and (3) to find the correlations between MSI and adsorption ability of NiM/MgO to CO_2.

2. Computational details

2.1. Computational method

All the calculations are performed in the framework of DFT by using the Cambridge Sequential Total Energy Package (CASTEP) [33,34]. The generalized gradient approximation (GGA) has been chosen to represent the exchange-correlation potential in the formulation of the Perdew–Burke–Ernzerhof (PBE) [35]. In this framework, a large convergence of the plane wave expansion is obtained with an energy cut off of 340 eV. For geometry optimization, the Brillouin zone is sampled in a $2 \times 2 \times 1$ Monkhorst-Pack set [36], and test calculations with a k-point grid of $5 \times 5 \times 1$ gave a numerical difference in Ni-M (M = Mn, Fe, Co, and Cu) binding energy of less than 0.01 eV. A Fermi smearing of 0.1 eV is utilized. The geometries are optimized, until the energy, the force and the max displacement converged to 2.0×10^{-5} eV/atom, 0.05 eV/Å and 2×10^{-3} Å, respectively. Spin polarization is considered throughout all calculations. All of the bimetals containing NiMn, NiFe, NiCo and NiCu are in high-spin states, and the initial magnetic moments of Mn, Fe, Co, Ni and Cu are 5.0, 4.0, 3.0, 2.0 and 1.0 uB, respectively.

The binding energy of NiM is evaluated according to the following formula:

$$E_{bin} = E_{NiM/MgO} - E_{NiM} - E_{MgO}$$

where $E_{NiM/MgO}$ is the total energy of the whole system, E_{NiM} and E_{MgO} are the energies of the isolated metal and support, respectively.

The adsorption energy of CO_2 is defined as follows:

$$E_{ads} = E_{CO_2-NiM/MgO} - E_{CO_2} - E_{NiM/MgO}$$

where $E_{CO_2-NiM/MgO}$ and E_{CO_2} represent the total energy of CO_2 adsorbing on NiM/MgO and the energy of the free CO_2, respectively. The energies of free NiM and CO_2 are computed by placing them in a 10 Å × 10 Å × 10 Å cubic box, respectively.

2.2. Model

Model about supported Ni-based catalyst is built based on two sections: the active component and the support.

(a) The active component

Ni-based bimetals (NiMn, NiFe, NiCo and NiCu) are described by two linking atoms (Ni-M).

(b) The support

In the following study, we select the stable surface of MgO, (1 0 0) surface, as the support. The lattice constant of MgO (1 0 0) is calculated to 4.301 Å with the error of 2.13% compared to the experimental value of 4.213 Å, which is in agreement with other DFT-based theoretical reports [37]. We model the MgO (1 0 0) surface using a four-layer slab. Meanwhile, we test the effect of the slab thickness on the energy data, and find that the binding energies change obviously going from three to four MgO layers, while they change at most by 0.01 eV in the same way from four to five, which proves the convergence versus slab thickness.

The calculations being periodic in three dimensions, we impose a vacuum of 10 Å between two consecutive slabs in order to eliminate any noticeable interaction with the periodic image along the z direction. Considering adsorptions of isolated bimetallic alloys, we use a 2×2 supercell containing 16 O and 16 Mg atoms, depicted in Fig. 1(a) and (b). Hence, the distance between two adsorbed NiMn is 6.083 Å (take NiMn as an example), which is large enough to prevent any noticeable lateral interaction. The formation of oxygen vacancy on the MgO (1 0 0) surface has been investigated in several previous theoretical studies by removing a neutral oxygen atom [27,38], as shown in Fig. 1(c). The bottom two layers are frozen in their bulk positions, whereas the remaining two layers together with NiM and the adsorbed CO_2 are allowed to relax in all calculations.

We consider that MSI exists when NiM adsorbs on surface.

3. Results and discussion

3.1. Interactions of NiM (Mn, Fe, Co, Cu) with MgO (1 0 0)

For the perfect MgO (1 0 0) surface, it is well known that the anionic site is the preferred adsorption site for most transition metal atoms [39]. For the oxygen vacancy surface, the transition metal atoms like to be adsorbed above the vacancy [28,40]. Therefore, in this work, we assume that Ni (or M) is adsorbed on oxygen atom for the perfect surface, while it is adsorbed above the oxygen vacancy for the defective surface, and the bond axis of NiM is perpendicular, parallel or oblique to the surface. The calculated results show that the adsorption structures of parallel state are most stable as shown in Fig. 2, and have been selected as the substrates, on which the CO_2 adsorption will be studied. The most stable adsorption modes are named as P (NiM) and D (NiM), with P indicating the perfect surface and D indicating the defective surface. For example, P (NiMn) and D (NiMn) represent the most stable configurations for NiMn supported on the perfect and defective surfaces. In P (NiMn), NiMn is with Mn and Ni atoms linking to two O atoms separately. In D (NiMn), NiMn is with Ni above the oxygen vacancy and Mn linking to O atom. Like NiMn, NiFe and NiCo occupy the same stable sites. However, the most stable adsorption configuration for D (NiCu) is with Cu above the oxygen vacancy and Ni linking to O atom.

Table 1
Binding energies (eV) of NiM adsorbing on MgO surfaces.

	NiMn	NiFe	NiCo	NiCu
P	−1.82	−1.83	−1.89	−1.83
D	−2.86	−2.99	−3.04	−3.02

3.1.1. Energetic analysis of NiM on MgO (1 0 0) surface

The interactions between NiM and MgO can be measured by binding energies of NiM on MgO, which have been shown in Table 1.

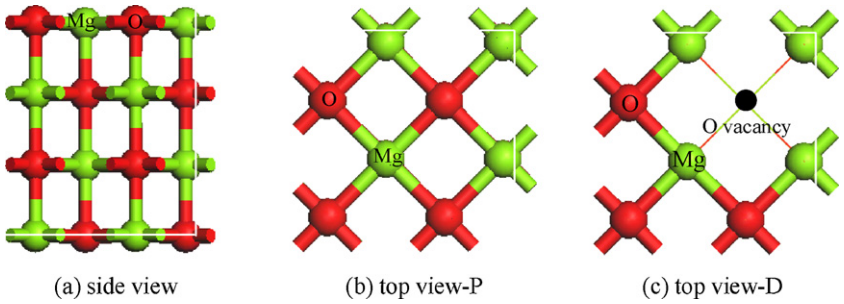

Fig. 1. Structures of top view of MgO (1 0 0) surface, side view of perfect and defective MgO surfaces (P represents the perfect surface and D is the defect surface).

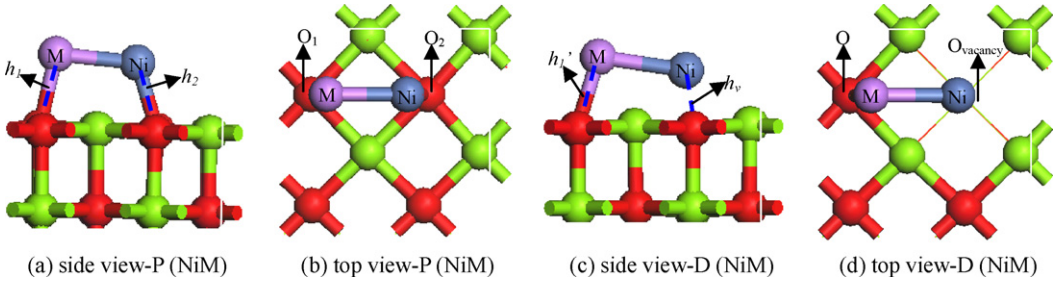

Fig. 2. The most stable configurations for NiMn adsorbing on perfect and defective surfaces, and the settings of the binding height for NiMn adsorbing on the two surfaces (h_1 as the distance between M and O_1 atom on the perfect surface, h_2 as the distance between Ni and O_2 atom on the perfect surface, h_1' as the distance between M and the O atom on the defect surface and h_v as the distance between Ni and the oxygen vacancy).

The calculated binding energies of NiM adsorbing on the perfect surface are −1.82, −1.83, −1.89 and −1.83 eV for bimetals along the row, namely NiMn, NiFe, NiCo and NiCu, respectively, and are −2.86, −2.99, −3.04 and −3.02 eV on oxygen vacancy, respectively. These results indicate that bimetals bind more strongly to the surface with oxygen vacancy than those to a perfect surface, which has been proved by theoretical studies combined with experimental detection [23,27,41,42].

In each MgO systems, although the differences of binding energies of different NiM bimetals are little, they can still exhibit the differences of the interactions between different bimetals NiM and MgO. Therefore, we distinguished the interactions by comparing the values of the binding energies. For the perfect surface, the order of binding energies is as follows: P (NiCo) > P (NiFe) = P (NiCu) > P (NiMn), and the binding energies of NiM adsorbing on the defective surface follow the sequence of D (NiCo) > D (NiCu) > D (NiFe) > D (NiMn). Clearly, both the two surfaces exhibit the strongest interaction with NiCo.

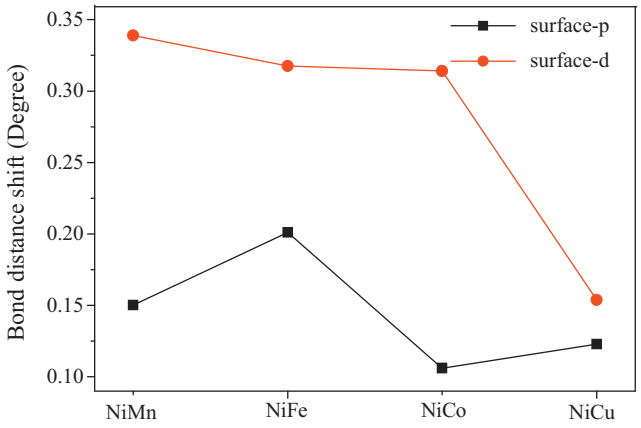

Fig. 3. The bond distance shift of NiM adsorbing on the two surfaces.

3.1.2. *Geometry analysis of NiM on MgO (1 0 0) surface*

The binding energies of these bimetals show an interesting correlation with their binding structures (bond distance shift, Δd, and binding heights, h). We defined Δd as the bond distance shift before and after the bindings of NiM. For binding heights, h, h_1 is considered as the distance between M and O_1 atom on the perfect surface, h_2 as the distance between Ni and O_2 atom on the perfect surface, h_1' as the distance between M and the O atom on the defective surface and h_v as the distance between Ni and the oxygen vacancy, as shown in Fig. 2.

In order to clarify the correlation between binding energies and binding structures, we plot the Figs. 3 and 4. For NiM bond distances, they are all lengthened after NiM adsorbing on the surfaces. From Fig. 3, it can be seen clearly that the bond distances of bimetals are extended more largely by the surface with oxygen vacancy than those by the perfect surface in all cases. For binding heights, from Fig. 4, we can see that h_v changes much compared to h_2, and the value of h_v is smaller than that of h_2, while h_1' does not show

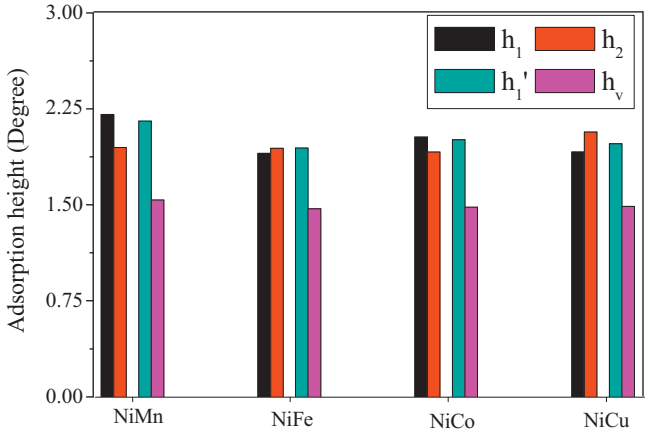

Fig. 4. The adsorption height of NiM adsorbing on the two surfaces.

Table 2
The Mulliken charges of NiM transferred from MgO (1 0 0).

	NiMn	NiFe	NiCo	NiCu
P	−0.30	−0.35	−0.34	−0.53
D	−0.68	−0.71	−0.73	−1.14

apparent changes compared to h_1. It is not difficult to understand that bimetals adsorb closer to the surface with oxygen vacancy than those to the perfect surface in all cases. Analyzing the above results, we can conclude that oxygen vacancy surface exhibits stronger interaction with the bimetals than the perfect surface does, which is consistent with the result gotten from the binding energies.

It is noted that no apparent trend of change can be got from the geometrical variations in each MgO system with different bimetals.

3.1.3. Electron analysis of NiM on the perfect and defective MgO (1 0 0) surfaces

It is understood that ultimately all catalytic effects must be electronic in the sense that chemical bonds are being formed and broken by the catalyst, and these bonds are electronic by nature [43]. In other words, the observed relationships greatly depend on the degree of electrons transfer between NiM and MgO (1 0 0). Therefore, in order to profound insight into the trends of the interactions between bimetals and MgO surface, the Mulliken charges are shown in Table 2.

According to the results listed in Table 2, several conclusions can be obtained. Firstly, the Mulliken charges of NiM adsorbing on the perfect and defective surfaces are both negative, indicating the electrons transfer from MgO surface to NiM upon chemisorption. Secondly, the data show a significant charges (−0.68 to −1.14e) transferred to NiM from the defective surface, which are more than that (−0.3 to −0.53e) from the perfect surface, indicating the defective surface attracts NiM stronger than the perfect surface, which is consistent with the results obtained from the binding energies. Thirdly, both on the perfect and defective surfaces, the transferred charges are increased gradually from NiMn to NiCu in the light of the sequence of the periodic table, which is consistent with the sequence of the binding energies of NiMn, NiFe and NiCo, except NiCu. NiCu attracts the most electrons owing to the fact that Cu has the half-filled $4s^1$ and $3d^{10}$ configurations.

3.2. Adsorption of CO_2 on supported NiM

3.2.1. Adsorption characteristics of CO_2 adsorbing on the substrate

Different CO_2 adsorption configurations on NiM/MgO substrates are explored and two adsorption configurations are found to be stable as shown in Fig. 5. We select the most stable one to study, as shown in Figs. 5(a) and (b). The most stable configurations for the two substrates are named as P (NiM)-CO_2 and D (NiM)-CO_2. For example, P (NiMn)-CO_2 and D (NiMn)-CO_2 represent the most stable configurations for CO_2 adsorbing on the perfect and defect substrates. For clarity, the oxygen atoms of CO_2 are labeled as O_a and O_b, CO_2 adsorbs directly on the NiMn with C atom linking to the bimetal, O_a linking to Mn atom and O_b linking to Ni atom.

The adsorption energies (E_{ads}) as well as other structural parameters of the configurations are summarized in Table 3.

In P (NiMn)-CO_2, the adsorption energy of CO_2 is −1.38 eV, C—O_a(O_b) bond is 1.286 (1.276) Å, and O_a—C—O_b angle is 129.2°. In D (NiMn)-CO_2, the adsorption energy of CO_2 is larger (−1.51 eV), C—O_a and C—O_b bonds are shorter, and O_a—C—O_b angle is larger compared to those of the former. The results show that D (NiMn) exhibits stronger adsorption ability to CO_2 than P (NiMn) does. However, in other three bimetals systems, the substrates with oxygen vacancy show the opposite action on the adsorption of CO_2.

Table 3
Bond distance (Å), the angle $\angle O_aCO_b$ of CO_2 (°) and adsorption energies of CO_2 (eV).

	C—O bond				$\angle O_aCO_b$		E_{ad}	
	C—O_a		C—O_b					
	P	D	P	D	P	D	P	D
NiMn	1.286	1.285	1.276	1.259	129.2	132.3	−1.38	−1.51
NiFe	1.284	1.288	1.268	1.262	132.8	132.0	−2.03	−2.01
NiCo	1.282	1.285	1.268	1.261	132.4	132.0	−2.11	−2.03
NiCu	1.230	1.264	1.300	1.267	129.9	135.0	−1.50	−1.41

For example, the calculated E_{ads} of CO_2 in P (NiFe)-CO_2 is −2.03 eV with O_a—C—O_b angel being 132.8°, while in D (NiFe)-CO_2, the E_{ads} value is smaller (−2.01 eV), and the O_a—C—O_b angel value is also smaller compared to those in P (NiFe)-CO_2. Therefore, one can conclude that the perfect substrate acts favoring the NiM—CO_2 bond, and NiM/MgO with oxygen vacancy weakens CO_2 adsorption. The fact of the adsorption energies of CO_2 decrease is consistent with experimental and theoretical results [37,44,45]. The reason that P (NiMn) system adsorbs CO_2 weaker than D (NiMn) system may be that NiMn bond in the perfect system is elongated apparently from 2.131 to 3.150 Å by the adsorption of CO_2, while NiMn bond in defect system as well as the other NiM bonds in each system is almost not changed.

We also compare the effects of each MgO system with different bimetals on the adsorption of CO_2. The calculated E_{ads} values of CO_2 follow the orders of P (NiCo)-CO_2 > P (NiFe)-CO_2 > P (NiCu)-CO_2 > P (NiMn)-CO_2 and D (NiCo)-CO_2 > D (NiFe)-CO_2 > D (NiMn)-CO_2 > D (NiCu)-CO_2, indicating the strongest adsorption ability of NiCo/MgO substrates to CO_2. In Section 3.1.1, we have found that D (NiCu) system shows higher binding energies than that in D (NiMn) and D (NiFe) systems, and NiCu obtains the most electrons because of the half-filled $4s^1$ and $3d^{10}$ configurations of Cu. Just because of this, D (NiCu) exhibits the relatively lower adsorption ability to CO_2 than D (NiMn) and D (NiFe) do.

3.2.2. Energetic analysis of CO_2 adsorbing on the substrate

Several studies [46,47] have stated that the adsorption of CO_2 can be considered as a two-step process: first, CO_2 deforms from its linear gas phase structure into a bent CO_2 fragment (distortion energy, $E_{def.CO_2}$); second, the bent CO_2 fragment binds the substrate (interaction energy, E_{int}), which is the driving force of the chemisorptions process, and can express the binding capability of the substrate. Of course, there is a deformation for the substrate in CO_2 adsorption ($E_{def.NiM/MgO}$). The adsorption energy of CO_2 on the substrate can be decomposed into deformation energy of CO_2, the deformation energy of the substrate and interaction energy between CO_2 and the substrate. Therefore, the E_{ads} of CO_2 can be expressed according to

$$E_{ads} = E_{int} + E_{def.NiM/MgO} + E_{def.CO_2}$$

The calculated $E_{def.CO_2}$, $E_{def.NiM/MgO}$ and E_{int} are listed in Table 4. Seen from Table 4, the data shows clearly that $E_{def.CO_2}$ and $E_{def.NiM/MgO}$ values are much smaller than E_{int} values and have no

Table 4
The distortion energies (eV) of CO_2 and the substrate as well as interaction energies (eV).

	$E_{dis\text{-}NiM}$		$E_{dis\text{-}CO2}$		E_{int}	
	P	D	P	D	P	D
NiMn	0.42	0.21	2.32	2.06	−4.16	−3.78
NiFe	0.29	0.14	2.07	2.10	−4.38	−4.26
NiCo	0.43	0.30	2.08	2.01	−4.61	−4.43
NiCu	0.08	0.039	2.21	1.82	−3.78	−3.28

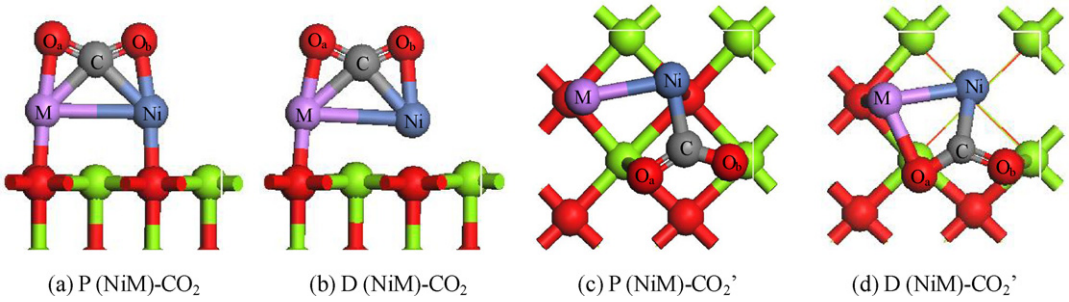

(a) P (NiM)-CO_2 (b) D (NiM)-CO_2 (c) P (NiM)-CO_2' (d) D (NiM)-CO_2'

Fig. 5. Stable configurations for CO_2 on perfect and defective substrates.

deciding effect on CO_2 adsorption, although they make contribution to the process of CO_2 adsorption. Therefore, we analyze E_{int} values only. The calculated E_{int} on the perfect substrates are −4.16, −4.38, −4.61 and −3.78 eV for bimetals systems along the row, namely NiMn, NiFe, NiCo and NiCu, respectively, and are −3.78, −4.26, −4.43 and −3.28 eV for the defect substrates. The results indicate that the existence of oxygen vacancy does not increase the binding ability of the substrate to CO_2, but decrease the binding ability compared to the perfect substrates, which is agreement with the conclusion gotten from adsorption energy except that of NiMn system. That is to say, the adsorption energy can be reflected well by interaction energy.

Similarly, the effects of each MgO surface system with different bimetals on the binding ability of the substrates to CO_2 have also been analyzed. According to the results exhibited in Table 4, the calculated E_{int} follows the orders of D (NiCo)-CO_2 > D (NiFe)-CO_2 > D (NiMn)-CO_2 > D (NiCu)-CO_2 and P (NiCo)-CO_2 > P (NiFe)-CO_2 > P (NiMn)-CO_2 > P (NiCu)-CO_2. Clearly, among the four bimetal systems, NiCo substrate shows the largest binding ability to CO_2, which is also consistent with the conclusion gotten from adsorption energy. The high degree of consistency between E_{int} values and E_{ads} values proves that the binding ability of the substrate to CO_2 decides the adsorption ability of the substrate to CO_2.

4. Conclusions

In this work, we conduct a DFT-based computational study on the interactions of NiM (M = Mn, Fe, Co and Cu) with perfect and defective MgO (1 0 0) as well as the effects of the interactions on the adsorption of CO_2. DFT calculations show that the binding energies of NiM on the oxygen vacancy are larger than those on the perfect surface, transferred charges between NiM and the defective surface are also larger than those between NiM and the perfect surface, which indicate the existence of oxygen vacancy increases the interactions between NiM and MgO (1 0 0) surface significantly. However, the removal of oxygen shows the weaker CO_2 chemisorptions on NiFe/MgO, NiCo/MgO and NiCu/MgO than the perfect substrates do. But NiMn/MgO defect system shows the higher adsorption ability to CO_2.

For each MgO system with different bimetals, the binding energies of NiM adsorbing on MgO (1 0 0) increase gradually from NiMn to NiCo system and then depress for NiCu system. The transferred charges follow the same order like the binding energies for NiMn, NiFe and NiCo systems except NiCu. Interestingly, the adsorption ability of CO_2 adsorbing on NiM/MgO substrates also follows the same order like the binding energies for NiMn, NiFe and NiCo, except NiCu. Among the four bimetal systems, NiCo shows the highest interaction with the surface, leading to the strongest CO_2 chemisorption both on the perfect and defect substrates.

Analyzing the connection between E_{bin} and E_{ads}, we can find that for the same bimetal systems with different MgO surfaces, the stronger the MSI is, the weaker the adsorption ability of the substrate to CO_2 is, except NiMn system, while for each MgO system with different bimetals, the stronger the MSI is, the stronger the adsorption ability of the substrate to CO_2 is, except NiCu system.

Acknowledgements

The work was supported financially by the National Basic Research Program of China (Grant no. 2005CB221203), the National Natural Science Foundation of China (no. 20976115) and the National Younger Natural Science Foundation of China (Grant no. 20906066).

References

[1] K. Tomishige, Y.G. Chen, K. Fujimoto, Journal of Catalysis 181 (1999) 91–103.
[2] J.R. Rostrup-Nielsen, J.H.B. Hansen, Journal of Catalysis 144 (1993) 38–49.
[3] A. Erdöhelyi, J. Cserényi, F. Solymosi, Journal of Catalysis 141 (1993) 287–299.
[4] O. Tokunaga, Y. Osada, S. Ogasawara, Fuel 68 (1989) 990–994.
[5] J.H. Kim, D.J. Suh, T.J. Park, K.L. Kim, Applied Catalysis A: General 197 (2000) 191–200.
[6] R. Takahashi, S. Sato, T. Sodesawa, M. Kato, S. Takenaka, S. Yoshida, Journal of Catalysis 204 (2001) 259–271.
[7] S. Tang, L. Ji, J. Lin, H.C. Zeng, K.L. Tan, K. Li, Journal of Catalysis 194 (2000) 424–430.
[8] V.C.H. Kroll, H.M. Swaan, C. Mirodatos, Journal of Catalysis 161 (1996) 409–422.
[9] H.M. Swaan, V.C.H. Kroll, G.A. Martin, C. Mirodatos, Catalysis Today 21 (1994) 571–578.
[10] A. Slagtern, Y. Schuurman, C. Leclercq, X. Verykios, C. Mirodatos, Journal of Catalysis 172 (1997) 118–126.
[11] H.Y. Liu, R.G. Zhang, F.Y. Ding, R.X. Yan, B.J. Wang, K.C. Xie, Applied Surface Science 257 (2011) 9455–9460.
[12] J.H. Sinfelt, Accounts of Chemical Research 10 (1977) 15.
[13] D. Bazin, C. Mottet, G. Treglia, Applied Catalysis A: General 200 (2000) 47–54.
[14] F. Besenbacher, I. Chorkendorff, B.S. Clausen, B. Hammer, A.M. Molenbroek, J.K. Nørskov, I. Stensgaard, Science 279 (1998) 1913–1915.
[15] A.M. Molenbroek, J.K. Nørskov, B.S. Clausen, Journal of Physical Chemistry B 105 (2001) 5450–5458.
[16] D. Liu, W.N.E. Cheo, Y.W.Y. Lim, A. Borgna, R. Lau, Y. Yang, Catalysis Today 154 (2010) 229–236.
[17] J.G. Zhang, H. Wang, A.K. Dalai, Journal of Catalysis 249 (2007) 300–310.
[18] J.T. Li, M.D. Chen, Q.G. Yan, H.L. Wan, I.R. TSA, Chemical Journal of Chinese Universities-Chinese 21 (2000) 1445–1447.
[19] E. Ruckenstein, Y.H. Hu, Applied Catalysis A: General 133 (1995) 149–161.
[20] Z. Xu, Y. Li, J. Zhang, L. Chang, R. Zhou, Z. Duan, Applied Catalysis A: General 210 (2001) 45–53.
[21] M.C.J. Bradford, M.A. Vannice, Catalysis Today 50 (1999) 87–96.
[22] Z.X. Yang, R.Q. Wu, Q.M. Zhang, D.W. Goodman, Physical Review B 65 (2002) 155407.
[23] A.D. Vitto, G. Pacchioni, F. Delbecq, P. Sautet, Journal of Physical Chemistry B 109 (2005) 8040–8048.
[24] S. Abbet, A. Sanchez, U. Heiz, W.D. Schneider, A.M. Ferrari, G. Pacchioni, N. Rösch, Journal of the American Chemical Society 122 (2000) 3453–3457.
[25] A. Sanchez, S. Abbet, U. Heiz, W.D. Schneider, H. Häkkinen, R.N. Barnett, U. Landmann, Journal of Physical Chemistry A 103 (1999) 9573–9578.
[26] S. Fernandez, A. Markovits, C. Minot, Chemical Physics Letters 463 (2008) 106–111.
[27] Y. Wang, E. Florez, F. Mondragon, T.N. Truong, Surface Science 600 (2006) 1703–1713.
[28] A.M. Ferrari, L. Giordano, G. Pacchioni, S. Abbet, U. Heiz, Journal of Physical Chemistry B 106 (2002) 3173–3181.

[29] S. Abbet, A. Sanchez, U. Heiz, W.D. Schneider, Journal of Catalysis 198 (2001) 122–127.
[30] A.M. Ferrari, L. Giordano, N. Rösch, U. Heiz, S. Abbet, A. Sanchez, G. Pacchioni, Journal of Physical Chemistry B 104 (2000) 10612–10617.
[31] S.A. Fuente, P.G. Belelli, R.M. Ferullo, N.J. Castellani, Surface Science 602 (2008) 1669–1676.
[32] A.R. Jose, M. Amitesh, The Journal of Phusical Chemistry 104 (2000) 3630–3638.
[33] M.C. Payne, D.C. Allan, T.A. Arias, J.D. Joannopoulos, Reviews of Modern Physics 64 (1992) 1045–1097.
[34] V. Milman, B. Winkler, J.A. White, C.J. Pickard, M.C. Payne, E.V. Akhmatsakaya, R.H. Nobes, International Journal of Quantum Chemistry 77 (2000) 895–910.
[35] J.P. Perdew, K. Burke, M. Ernzerhof, Physical Review Letters 77 (1996) 3865–3868.
[36] H.J. Monkhorst, J.D. Pack, Physical Review B 13 (1976) 5188–5192.
[37] D.R. Alfonso, J.A. Snyder, J.E. Jaffe, A.C. Hess, M. Gutowski, Physical Review B 62 (2000) 8318–8322.
[38] A. Bogicevic, D.R. Jennison, Surface Science 437 (1999) L741–L747.
[39] I. Yudanov, G. Pacchioni, K. Neyman, N. Rösch, Journal of Physical Chemistry B 101 (1997) 2786–2792.
[40] J.W. He, P.J. Moller, Surface Science 180 (1987) 411–420.
[41] S. Abbet, E. Riedo, H. Brune, U. Heiz, A.M. Ferrari, L. Giordano, G. Pacchioni, Journal of the American Chemical Society 123 (2001) 6172–6178.
[42] L. Giordano, G. Pacchioni, F. Illas, N. Rösch, Surface Science 499 (2002) 73–84.
[43] G.L. Haller, D.E. Resasco, Advances in Catalysis 36 (1989) 173–235.
[44] J.H. Kang, E.W. Shin, W.J. Kim, J.D. Park, S.H. Moon, Journal of Catalysis 208 (2002) 310–320.
[45] F. Morales, E. de Smit, F.M.F. de Groot, T. Visser, B.M. Weckhuysen, Journal of Catalysis 246 (2007) 91–99.
[46] Y.X. Pan, C.J. Liu, T.S. Wiltowski, Q.F. Ge, Catalysis Today 147 (2009) 68–76.
[47] M.C. Valero, P. Raybaud, P. Sautet, Journal of Catalysis 247 (2007) 339–355.